MACROSCOPIC FAILURE DUE TO BALLISTIC TESTS

The main difference between penetration into a semi-infinite target and perforation of a single-plate target is the interaction of the rod with the rear free surface of the plate. The rod is only interacting with the target by its momentary tip, and it is reduced in length and velocity during its penetration process. No bulging occurs (fig. 17).

Figure 17: Semi-infinite target

Bulging occurs when the tip of the rod comes close to the backside. The resistance of the plate against penetration decreases during the late phase. This behavior is responsible for the fact that the penetration depth in a semi-infinite target is smaller than the ballistic limit thickness of a single-plate target. Fig. 18 shows the crater of a short cylinder projectile with L/D =1 in a steel plate near ballistic limit loading. The damage demonstrates an example of plug formation [13]. This plug has to take in consideration for penetration models.

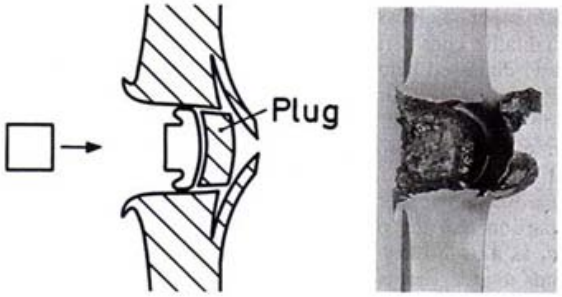

Figure 18: Crater of a short steel cylinder with plug formation

A penetration process involves various failure mechanisms which occur during the interaction of a rod or bullet and the armour material. The armour plates shown in fig. 19 are of intermediate thickness and realistic behavior can be simulated. The dimension of a realistic armour plate leads to perforation; this means all failure from the onset of penetration up to the damage of the back surface. The mechanisms have to taken in consideration for models.

The failure mode is influenced by geometry and materials behavior of the rods and plates. If the materials thermo mechanical properties favors the formation of shear bands plugging is very likely. In a brittle material fracture will be possible and it leads to discing failure.

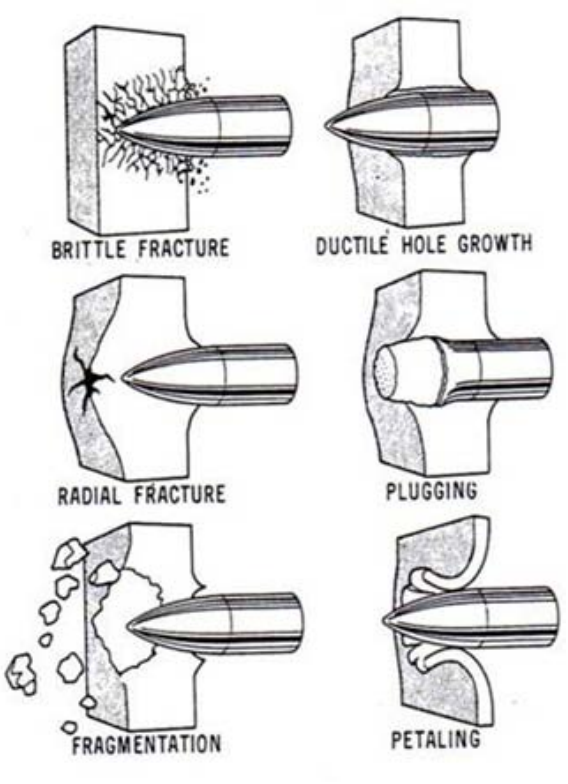

Figure 19: Possible failure modes in different impact situations [12]

EVALUATION OF BALLISTIC PERFORMANCE

PENETRATION: Characterized by a DoP (depth of penetration) test. Penetration in studied material and backing will be compared to the residual penetration in a semi infinite target (fig. 20). Information about: maximal ballistic protection potential, direct comparison of materials and „materials ranking".

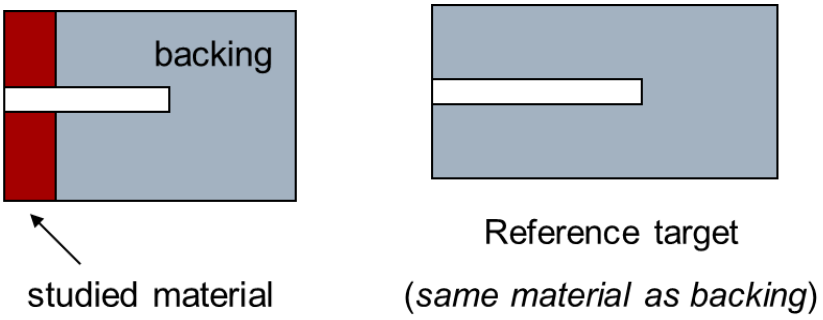

Figure 20: Test configuration to determine penetration

PERFORATION: Occurs at single target designs. Perforation is characterized by the ballistic limit velocity or the residual velocity. It gives information about the effective ballistic protection potential and the concerning realistic mass of a target or the mass of the system (fig. 21).

Another way to characterize perforation is a backing in a distance to the single armour plate. The residual penetration (fig. 21) indicates the terminal ballistic potential. Nowadays it is possible to measure exactly the residual velocity, so that this method is no more in use.

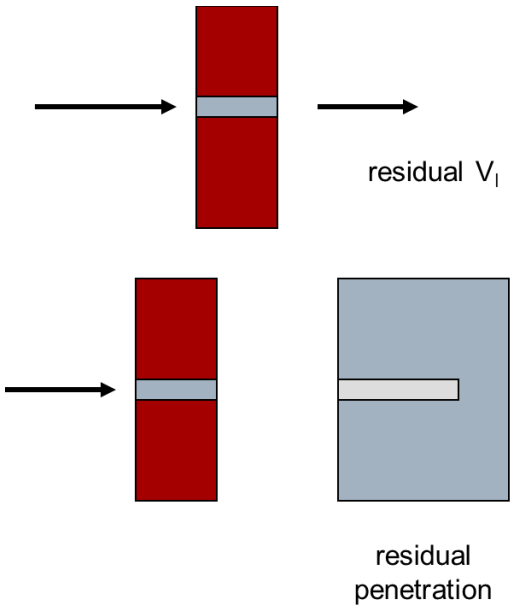

Figure 21: Test configuration to determine perforation

A: DoP (Depth of Penetration) test

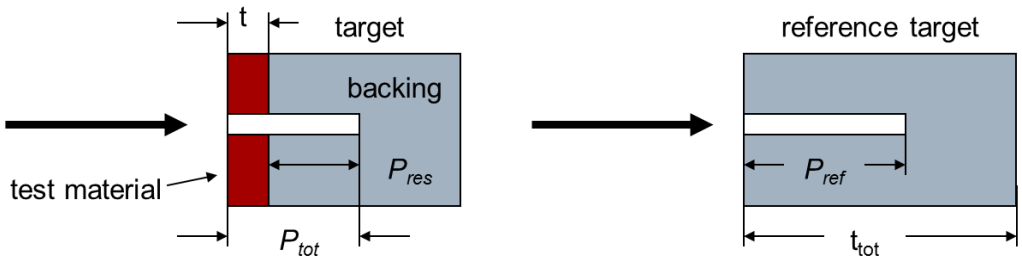

	effectiveness factor	equivalence factor
Volume	$E_s = \frac{P_{ref}}{P_{tot}}$	$F_s = \frac{t_{ref}}{t}$
Mass	$E_m = E_s \frac{\rho_{ref}}{\rho_{tot}}$	$F_m = F_s \frac{\rho_{ref}}{\rho}$

equivalence factor = evaluation of test material only
effectiveness factor = evaluation of both test material and backing

Figure 22: Test design and characteristic data of the DoP test.

The DoP test is used to compare the ballistic protection capability of different materials with a reference target. The backing of the studied material has to be the same as that of the reference target. It is aimed

to find out some parameter to characterize the influence of materials strength, toughness and density on the protection capability. The effectiveness factor (F) considers the studied material only and therefore the residual penetration in the backing is subtracted from penetration of the reference target. Contrariwise the effectiveness factor considers both test material and backing. Therefore the penetration depth P_{tot} is compared to the reference penetration. E_s and F_s indicate the influence on the volume and E_m and F_m on the mass of armour.

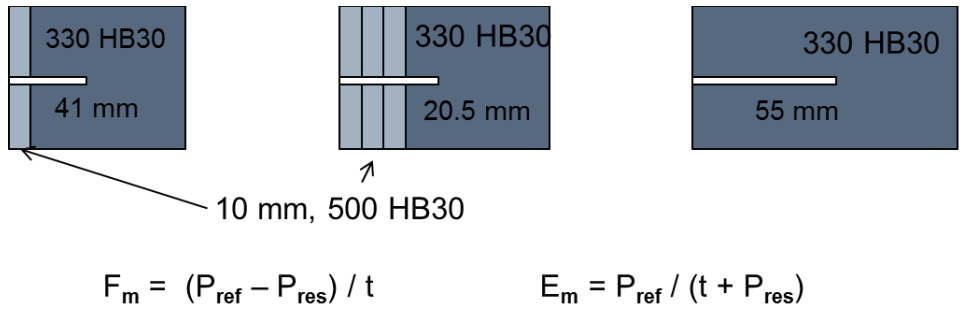

Figure 23: Test design with different test plate thickness

The values of equivalence and effectiveness factor can be easily manipulated by the quality of reference material and thickness of test material.

F_m –value for a test plate thickness of	10 mm	30 mm
	1.4	**1.15**
E_m-value for a test plate thickness of	10 mm	30 mm
	1.09	**1.08**

Fm-values are depending strongly on the thickness of studied materials. This fact has to be taken in consideration for an evaluation of the quality of armour material. The thickness of test plates for the E_m-value is of minor influence.

B: Ballistic Limit (V_{50})

The **ballistic limit** or **limit velocity** is the velocity, required for a particular projectile, to reliably (at least 50% of the time) penetrate a particular piece of material. In other words, a given projectile will not pierce a given target when the projectile velocity is lower than the ballistic limit [14]. The term *ballistic limit* is used specifically in the context of armour.

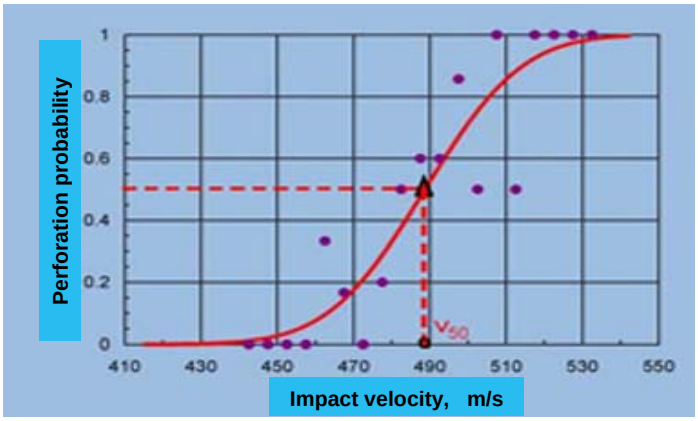

Figure 24: Gaussian distribution characterized by a mean value (v_{50} = ballistic limit v_{lim}) and Root mean square deviation

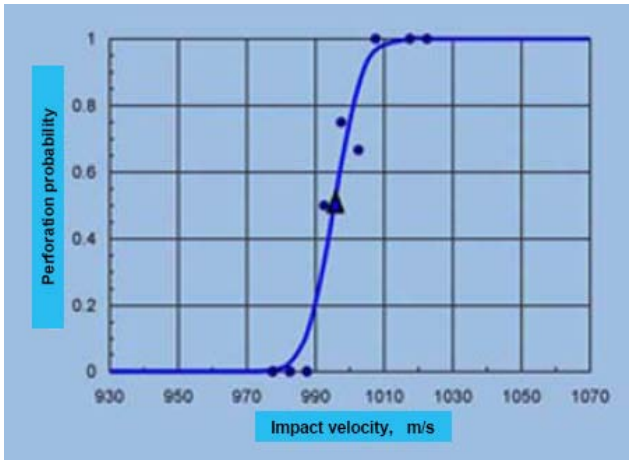

Figure 25: Example for a homogeneous material (a steel alloy)

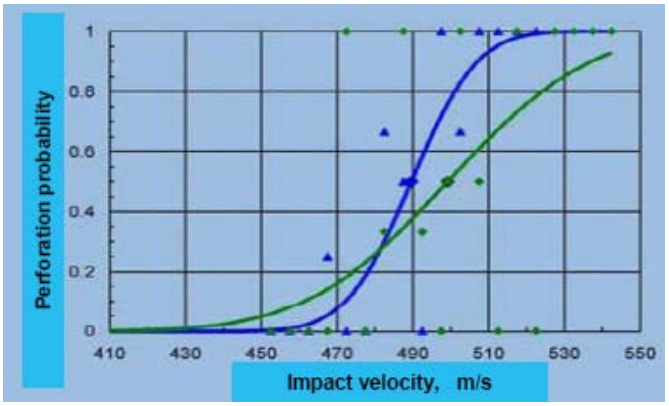

Figure 26: Example for heterogeneous material (composite). Protection is increased (higher V_{50}), but the curve is stronger decreased due to scattering of the results.

Homogeneous armour materials based on metals and ceramics may adequate tested by the V_{50} method with < 14 shots. For heterogeneous materials like fibre reinforced composites more shots (<30) are necessary. The standard deviation should be taken also in consideration.

MODELLING OF PENETRATION AND PERFORATION

Classical equations of perforation

The hypothesis of shear plugging assumes that the bullet is non deformable and the plate will be punched i. e. the materials are moving in axial direction only. At the interface between the target material and the plug dominates shear stress. Shear stress τ amounts to $\tau = 0.5\ \sigma$. It could be approximated as a pure punching process and described with equation (1):

$$F_{Shear}(x) = (t - x)\ D\ \pi\ \tau \qquad (1)$$

F_{Shear} = specific shear resistance, t = thickness of armour plate, x = penetration, D caliber of bullet, τ = shear resistance of armour plate (fig. 27 a))

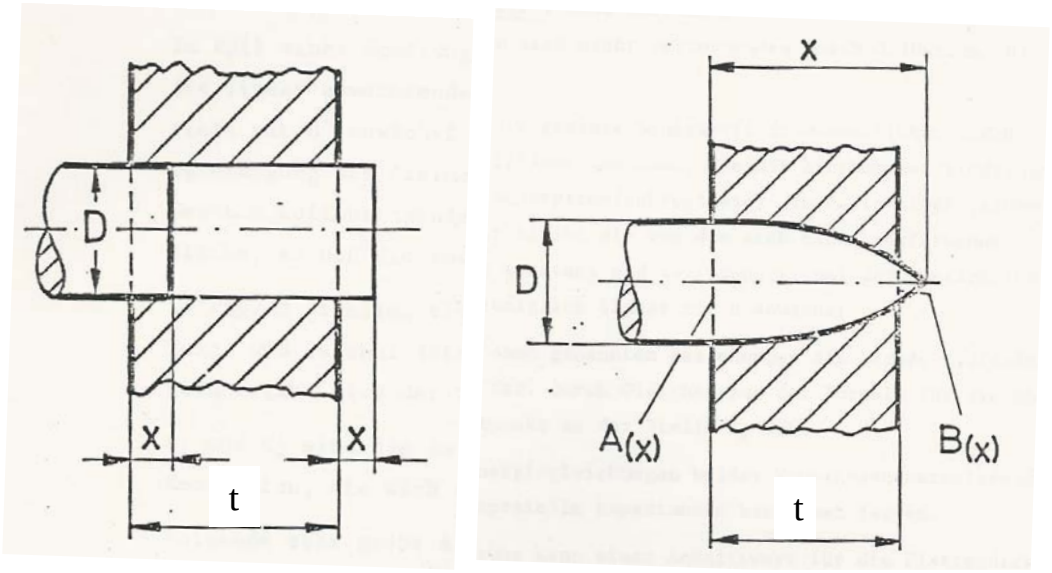

Figure 27 a) and b): Schematically presentation of shear plugging (a) and displacement of material (b)

The shear energy for the penetration is resulting from the integration of F_{Shear} (x) in the interval (0, t):

$$E_{Shear} = D\,\pi\,\tau \int_0^t (t-x)dx = D\,\pi\,\tau\,\frac{t^b}{2} = C_1\,D\,t^b \qquad (2)$$

b = 2 in equation (2). The factor C_1 represents the deformation resistance and inertia effects of the target plate. Based on this equation, considering shear resistance as an important influence on the ballistic capability, some scientist used different values for b depending on their experimental results [15]:

Noble : b = 2.035 for 250 mm $\leq$ t $\leq$ 500 mm
b = 1.654 for 100 mm $\leq$ t $\leq$ 250 mm

Hélie : b = ¾

Gâvre : b = 4/5

C_1 is constant for a specific b. Only Moisson [16] assumed C_1 depending from impact velocity by $C_1 = C' / v$.

Martel [17] assumed in his theory that for the penetration and perforation of a bullet the energy is proportional to the plastically displaced volume of target material (fig. 27 b)):

$$E_{dis}(x) = C\,V(x) \qquad (3)$$

x = penetration, V = displaced volume, E_{dis} = energy for displace material

A bullet having a diameter of D will lose the energy E_{dis} during a perforation of an armour plate with a thickness of t (equation (4)).

$$E_{dis} = C \pi \frac{D^2}{4} t = C_2 D^2 t \quad (4)$$

The resistance against penetration at x is given by a differentiation of E_{dis} to x:

$$F_{dis}(x) = dE_{dis}/dx = C\, dV(x)/dx = C\, A(x) \qquad \text{for } x \leq t \quad (5)$$

$$F_{dis}(x) = C[A(x) - B(x)] \qquad \text{for } x > t \quad (6)$$

A(x) and B(x) are cross sections of a bullet with the front side and the back side of a target plate. The factor C_2 represents like C_1 the deformation resistance and inertia effects of a target plate. If B(x) becomes equal to A(x) $F_{dis}(x)$ equals 0, i.e. there is no further loss of energy for the cylindrical part of the bullet during perforation. Equation (6) does not take frictional effects into account.

Comparison of the two hypotheses: shear deformation is characterized by a linear increasing surface of the bullet. The shear resistance increases with t^2. For poor displacement the resistance force is proportional to the cross section of the bullet and the resistance force stays constant. The energy increases linear with t.

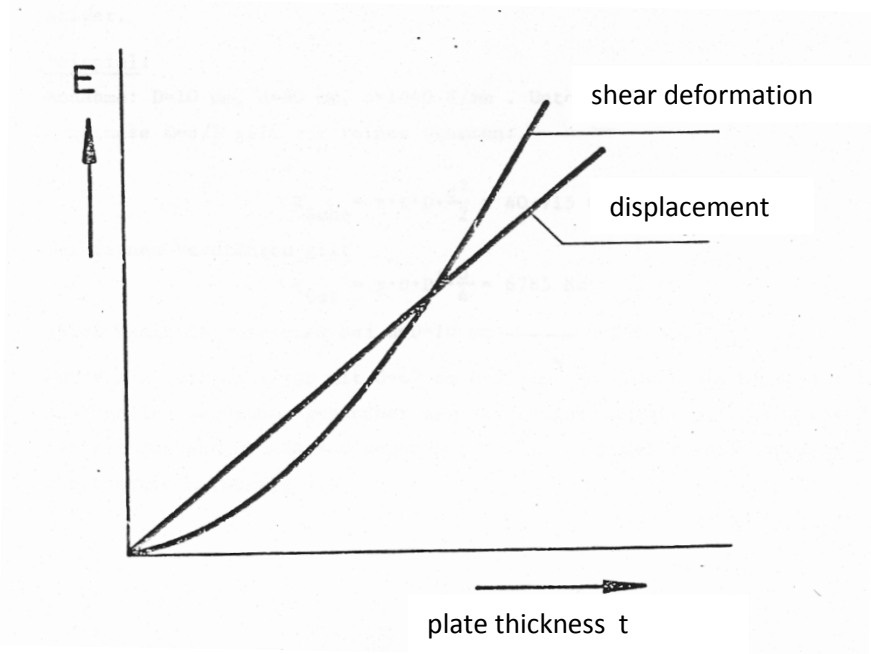

Figure 28:

For thin armour plates shearing is dominating, whereas for thicker plates displacing of target materials dominates the perforation as it is in fig. 28 characterized.

An acceptable approximation was achieved by a combination of the two equations:

$$E = A\, E_{Shear} + B\, E_{dis} = A\, C_1\, D\, t^2 + B\, C_2\, D^2\, t \quad (7)$$

A + B are factors for distribution.

The equation (7) with two terms was the base of some equations for perforation. For practical application the two terms of equation (7) were transformed in in one term:

$$E = C\ D^a\ t^b \tag{8}$$

$$a > 1,\quad b > 1,\quad a + b \approx 3$$

C depends on impact velocity, penetration velocity, shape of the bullet and the materials properties of the bullet and armour plates. Some equations based on this assumption. Among these equations the two most famous are these von Krupp [18] and de Marre [19]:

Krupp: $$E = B_1\ D^{5/3}\ t^{4/3} \tag{9}$$

de Marre: $$E = B_2\ D^{1.5}\ t^{1.4} \tag{10}$$

In the equation of de Marre the sum of the exponents amounts to 2.9.

The model of Tate and Alekseevskii for KE-Projectiles

For steady-state flow, neglecting materials compressibility and considering in the simplest case only one-dimensional flow, the *Bernoulli equation* (11) can be applied.

$$½\ \rho_P\ (v_P - u)^2 = ½\ \rho_T\ u^2 \tag{11}$$

In equation (11) ρ_P and ρ_T are the density of the projectile and the target, respectively. v_P = impact velocity, u = penetration velocity. Figure 27 shows a schematic diagram of the hydrodynamic penetration.

Based on physical facts an improvement of the hydrodynamic theory was expected by taking in account the dynamic strength of rod and target material [13]. This has been done by Alekseevskii [20] and Tate [21]. The equation of Tate and Alekseevskii (TA) is based on the equation of Bernoulli. Since the residual rod is decelerated during penetration by elastic wave reflection at its rear end, the TA equation (12) has to be fulfilled not only for the impact velocity v_P but also for each momentary residual velocity v and the corresponding penetration velocity u (fig. 27):

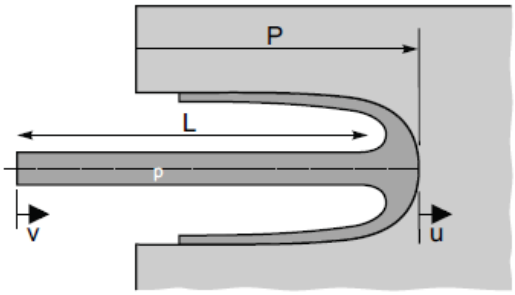

Figure 27: Schematic diagram of hydrodynamic penetration. P = length of the crater at time t, L= length of the rod
ρ = density, v = impact velocity, u = penetration velocity

$$½\ \rho_P\ (v - u)^2 + Y_P\ =\ ½\ \rho_T\ u^2\ + R_T \tag{12}$$

Cause of the deceleration of the rod during penetration, the material flow is not exactly stationary. But experimental investigations have been showing that the flow is most of the time nearly stationary and therefore called quasi-stationary flow.

The relative magnitudes of R and Y influence the penetration principally:

Case $R_T < Y_P$

In this case, there are two velocity regimes with different penetration processes. This is described by:

$$Y_P \leq \text{or} \geq \tfrac{1}{2} \rho_T u^2 + R_T \quad \{ \quad u = v_p \quad \text{or} \quad u < v_p \tag{13}$$

If Y_P is larger or equal to the right-hand side (13), the dynamic pressure at the tip of the rod cannot deform it, and the rod penetrates like a rigid body with $u = v_p$.

Figur 28: Penetration of a W sinter rod in P900 target. V_P = 1700 m/s, σ_{rod} = 1800 MPa, σ_{target} = 1200 MPa

The micrograph in fig. 28 shows the penetration of a W sinter rod at an impact velocity of 1700 m/s in a target consisting of P900. The dynamic strength of the rod amounts to 1800 MPa and that of the target material 1200 MPa. V_P in this example is slightly increased to u. After the test 70 % of the original rod length was found, so it could be roughly taken as a rigid body penetration. Hardness measurements revealed that the microstructure of the rod was strongly destroyed due to the toughness of the target material.

Case $R_T > Y_P$

In this case, there are also two velocity ranges. The dynamic pressure produced by the rod at the target increases with the velocity according to the left-hand side of (14):

$$\tfrac{1}{2} \rho_p v_p^2 + Y_P \leq \text{or} \geq R_T \quad \{ \quad u = 0 \quad \text{or} \quad u > 0 \tag{14}$$

Figure 29: Penetration of a W sinter rod in P900 target. V_P = 1700 m/s, σ_{rod} = 1800 MPa, σ_{target} = 2000 MPa

Penetration occurs only if the left-hand side of (14) becomes larger than R_T. For u = 0 no penetration occurs and the process is running like a Taylor test. If u > 0 penetration occurs. Fig. 20 shows a micrograph of a penetrated target consisting of P900. For this target the alloy was work hardened to the strength of 2000 MPa. The strength of the W sintered rod is slightly smaller and amounts to 1800 MPa. After the test only 20 % of the rod's original length was found. The hardness of the remaining rod was the same as of the original rod.

REFERENCES

1. http://www.frfrogspad.com/intballi.htm

2. Gonzalez Jr., Joe Robert (1990), Internal Ballistics Optimization, Thesis, AD-A225 791,

3. Horst, Albert W. (November 2005), *A Brief Journey Through the History of Gun Propulsion*, Aberdeen Proving Ground, MD: United States Army Research Laboratory, ARL-TR-3671

4. Ballistics at Encyclopædia Britannica Online, Accessed April 27, 2009

5. Carlucci, Donald E; Sidney S. Jacobson (2007). *Ballistics: Theory and Design of Guns and Ammunition*. CRC Press. p. 3. ISBN 1-4200-6618-8.

6. How do bullets fly? by Ruprecht Nennstiel, Wiesbaden, Germany

7. A Short Course in External Ballistics

8. Terminal Ballistics Test and Analysis Guidelines for the Penetration Mechanics Branch – BRL

9. Rosenberg, Z., Dekel, E., Terminal Ballistics, Springer, Heidelberg, 2012

10. http://mathscinotes.wordpress.com/2011/01/11/ballistics-ogives-and-bullet-shapes-part-1/

11. http://www.ruag.com/Ammotec/Defence_and_Law_Enforcement/9x19/Deformation_ammunition

12.Backman M. E., Terminal ballistics. Naval Weapons Center Report NWC-TP-5780. NWC China Lake, CA, 1976

13. Zukas J. A., High Velocity Impact Dynamics, Wiley, New York, 1990

14. Carlucci D. E., Jacobson S. S., *Ballistics: Theory and Design of Guns and Ammunition, CRC Press, 2008, p. 310*

15. G. Weihrauch et al.: "Anwendung klassischer Panzerformeln auf Wuchtgeschosse", ISL, 1979

16. Moisson: "Essai d'un mode d'.valuation de la r.sistance des plaques de blindage", M.morial de l'artillerie de la marine, tome XXIII, 1895

17. Martel, Mesure de la durete des metaux a la penetration au moyen d'empreintes … ., Comm. de methodes methodes d'essai, tome II, S.A., 1897

18. Krupp F: "Über das Durchschlagen von Panzerplatten", Essen, 1885 und 1888

19. de Marre J: .Perforation des toiles et plaques de fer et d'acier en tir normal. Memorial de l'artillerie de la marine, tome XIV, Paris, 1886

20. Alekseevkii V. P., Penetration of a Rod into a Target at High Velocity, Fiz. Goren, Vzryra, 2, 1966, p. 99

21. Tate A., A Theorie for the Deceleration of Long Rods After Impact, J. Mech. Phys. Solids, 17, 1967, p. 387